Soils and Foundations 2015;55(3):485–492

HOSTED BY

ELSEVIER

CrossMark

The Japanese Geotechnical Society

Soils and Foundations

www.sciencedirect.com
journal homepage: www.elsevier.com/locate/sandf

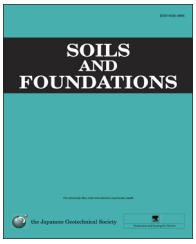

Analysis of stress and deformation of a positive buried pipe using the improved Spangler model

Yong Tian, Hao Liu*, Xue Jiang, Rangang Yu

College of Pipeline and Civil Engineering, China University of Petroleum (East China), Qingdao 266580, China

Received 13 November 2013; received in revised form 27 October 2014; accepted 28 November 2014
Available online 5 May 2015

Abstract

In the Spangler model, the vertical earth pressure is assumed to be uniformly distributed, but it is not. The aim of this study is to improve the accuracy of the stress and deformation calculation for a positive buried pipe by using the new formulae derived from an improved Spangler model. Based on the Spangler model, this study derives the general calculation formulae for the section moment of a buried pipe when the vertical earth pressure is arbitrarily distributed. Furthermore, this study proposes a new model by improving the Spangler model, in which the vertical earth pressure is assumed to be parabolically distributed. Then, the new deformation formulae are derived. At the end of this article, the results of the new formulae are validated through a comparison with the simulated results obtained by FLAC3D software. It is concluded that the new model can simulate the behavior of buried pipes better than the Spangler model.

Keywords: Buried pipe; Spangler model; Stress; Deformation; Formulae; FLAC3D

1. Introduction

Buried pipes are widely used for oil and gas transportation and for city pipe networks. Generally, in many countries of the world, the structural design of buried pipes is based on national standards. Those standards differ from one country to another, but most of them are based on the Marston–Spangler theory (Tian, 1989).

Many closed-form solutions for rigid pipes and culverts are subjected to earth load. Marston and Anderson (1913) first proposed a theory, and developed formulae that are widely used in practice, to estimate the vertical earth load on positive buried rigid pipes and culverts. The Marston model is shown in Fig. 1. Based on Marston's work, later researchers (Das and Seeley, 1975; Ladanyi and Hoyaux, 1969; Meyerhof and Adams, 1968; Matyas and Davis, 1983a; Vesic, 1971) made continuous improvements and developed formulae for the vertical earth load on rigid pipes and culverts. Among those formulae, the values for the soil lateral pressure coefficient (k) are different. The influence of soil cohesion and the plane of equal settlement are taken into consideration in some of the above theories, but not in others, as demonstrated (Tian, 1989). Furthermore, the shear plane is assumed to be the circular surface in Vesic's theory (Vesic, 1971) relative to the vertical shear plane in other theories. The above differences lead to different values for C_c in those theories.

Spangler (1941) conducted extensive research on flexible pipes. Analysis methods for stress and deformation were proposed and calculation formulae were developed. It is assumed that the vertical earth pressure and subgrade reaction are uniformly distributed on

*Corresponding author. Tel.: +86 150 6682 8856.
E-mail address: 821261214@qq.com (H. Liu).
Peer review under responsibility of The Japanese Geotechnical Society.

http://dx.doi.org/10.1016/j.sandf.2015.04.001

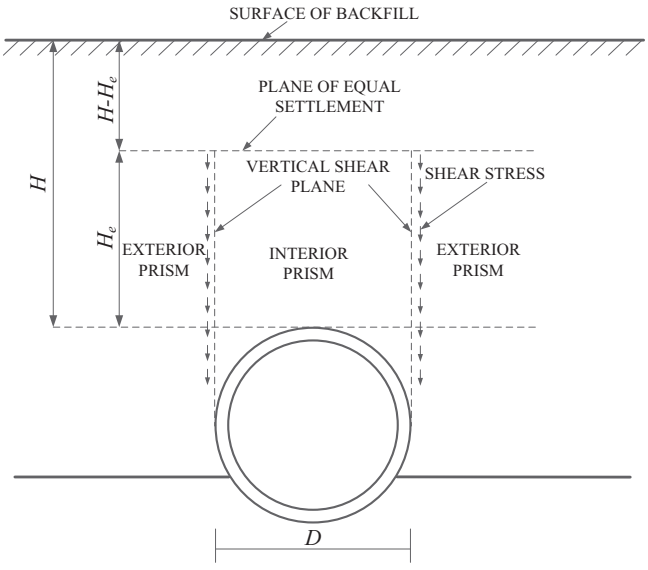

Fig. 1. Marston model.

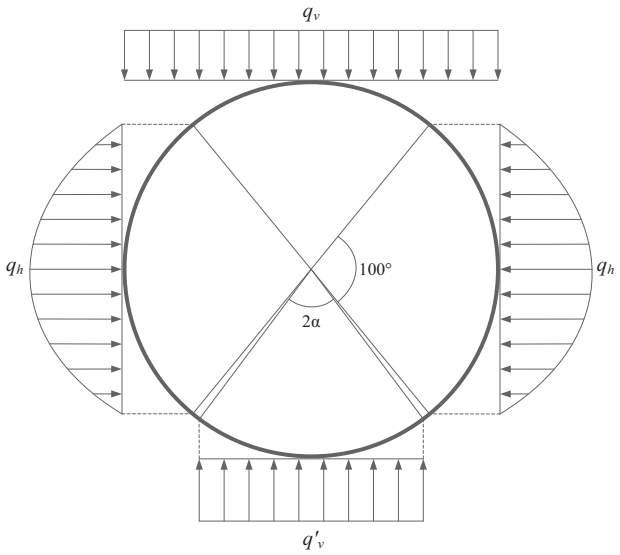

Fig. 2. Spangler model.

the pipe along its diameter. The lateral bearing resistance of soil was assumed to be parabolically distributed over a range of 100°. The Spangler model is shown in Fig. 2.

In the Marston – Spangler theory, the vertical earth pressure is assumed to be uniformly distributed. Actually, some experiments (Li, 2009; Shmulevich et al., 1986) indicate that the vertical earth pressure is not constant at different points on the pipe. Based on the Spangler theory, the aim of this study is to derive general calculation formulae for the section moment of a buried pipe when the vertical earth pressure ($q(x)$) is arbitrarily distributed. Then, the study assumes that the vertical earth pressure is parabolically distributed and derives the moment and deformation formulae for the purpose of obtaining higher calculation accuracy than with the Spangler formulae (Deng and Li, 1998; Spangler, 1941) through a comparison with the numerical values obtained by FLAC3D.

2. Vertical earth load

In Fig. 1, two imaginary vertical planes, known as shear planes Marston and Anderson (1913), are drawn tangent to the two sides of the pipe to define interior and exterior prisms. The plane of equal settlement is a special plane where the relative movement of the prisms is zero. H_e is the height of the plane. Since the deformation of the rigid pipe is nearly zero, the exterior prism moves downward, with respect to the interior prism, and the relative movement induces shear stresses on the shear planes. As a result, the earth load on the pipe is greater than the weight of the interior prism. According to the Marston theory Marston and Anderson (1913), the vertical earth load on rigid pipes can be determined from

$$W_e = C_c \gamma D^2 \tag{1}$$

where W_e is the vertical earth load per unit length of pipe, kN; γ is the unit weight of the backfill, kN/m^3; D is the outside diameter of the pipe, m; C_c is the load factor.

Marston and other researchers have given different solutions to C_c in their theories (Matyas and Davis, 1983b). Based on those theories, however, some simplified formulae are used in many design standards for buried pipes. For instance, Eq. (2) is adopted in "GB50332-2002, Structural design code for pipelines of water supply and waste water engineering" in China (Liu and Yang, 2001) and Eq. (3) is adopted in "USAS A21.1, USA Standard for Thickness Design of Cast Iron Pipe, Thickness Determination for Pipe on Piers or Piling Above Ground or Underground" (Matyas and Davis, 1983b).

$$C_c = 1.4\frac{H}{D} \tag{2}$$

$$C_c = 1.961\frac{H}{D} - 0.934 \tag{3}$$

Eq. (1) is suitable for rigid pipes and culverts, and the pipe – soil stiffness ratio should be taken into consideration when calculating the vertical earth load of flexible pipes (Tian, 1994). The formula can be given as

$$W = \xi W_e = \xi C_c \gamma D^2 \tag{4}$$

where ξ denotes the relative stiffness coefficient of the pipe, and the soil is expressed as follows:

$$\xi = \frac{E}{E_d}\left(\frac{\delta}{r}\right)^3 \tag{5}$$

where E is the elastic modulus of the pipe, MPa; E_d is the deformation modulus of backfill, MPa; δ is the thickness of pipe wall, m; r is the radius of the pipe, m.

3. General calculation formulae for section moment and stress

In this section, if the inner pipe wall is subjected to tension, the section moment is designated positive; if the outer pipe wall is subjected to tension, the section moment is designated negative.

3.1. Section moment produced by vertical earth pressure

When the vertical earth pressure ($q(x)$) is arbitrarily distributed, due to the symmetry of the structure and the pressure shown in Fig. 2, a simplified mechanical model can be applied, as shown in Fig. 3, under the vertical earth pressure and subgrade reaction. The length of the pipe ring is the unit length.

In Fig. 3(a), the resultant of $q(x)$ and q' is zero, and a relative displacement of points A and B occurs. Point B is selected as the reference point, whose displacement is zero, and the displacement of point A is the relative displacement. Therefore, Fig. 3(a) is equivalent to Fig. 3(b), which can be divided into two parts, as shown in Fig. 3(c) and (d). Removing the support restraint on point A in Fig. 3(c) and (d), a horizontal force and bending moment act on the point. In order to simplify the calculation formula for section moment, a rigid arm is introduced and the bending moment and the horizontal force can be transferred to the center of the circle (point O), that is, X_1 and X_2. During the calculation of the section moment of the pipe, the effect of X_1 and X_2 is delivered to the pipe through the rigid arm.

In Fig. 3(c), through a calculation with the force method, the values for X_1 and X_2 are expressed as follows:

$$X_1 = -\frac{1}{\pi}\int_0^{\pi} M_q(\theta)d\theta \tag{6a}$$

$$X_2 = -\frac{2}{\pi R}\int_0^{\pi} M_q(\theta)\cos\ \theta d\theta \tag{6b}$$

where $M_q(\theta)$ denotes the bending moment acting on the pipe ring, produced only by $q(x)$ and without X_1 and X_2; it is given by

$$M_q(\theta) = \begin{cases} -R^2\int_0^{\theta} q(R\ \sin\ t)\sin\ td(\sin\ t) & 0 \le \theta \le \pi/2 \\ -R^2\int_0^{\frac{\pi}{2}} q(R\ \sin\ t)\sin\ td(\sin\ t) + & \\ R^2(1-\ \sin\ \theta)\int_0^{\frac{\pi}{2}} q(R\ \sin\ t)d(\sin\ t) & \pi/2 \le \theta \le \pi \end{cases} \tag{7}$$

The section moment produced by the vertical earth pressure is

$$M_1(\theta) = X_1 + X_2 R\ \cos\ \theta + M_q(\theta)$$
$$= -\frac{1}{\pi}\int_0^{\pi} M_q(\theta)d\theta - \frac{2\ \cos\ \theta}{\pi}\int_0^{\pi} M_q(\theta)\cos\ \theta d\theta + M_q(\theta) \tag{8}$$

3.2. Section moment produced by subgrade reaction

The mechanical model is shown in Fig. 3(d). Using the analysis and the calculation method in Section 3.1, the section moment produced by the subgrade reaction is

$$M_2(\theta) = \begin{cases} \frac{RW}{12\pi}\left[3k_1(\alpha) - 2\sin^2\alpha\ \cos\ \theta\right] & 0 \le \theta \le \pi - \alpha \\ \frac{RW}{12\pi}\left[3k_1(\alpha) - 2\sin^2\alpha\ \cos\ \theta - 3\pi(\sin\ \alpha - \sin\ \theta)^2/\ \sin\ \alpha\right] & \pi - \alpha \le \theta \le \pi \end{cases} \tag{9}$$

where $k_1(\alpha)$ is given by

$$k_1(\alpha) = \alpha\ \sin\ \alpha + \frac{3}{2}\ \cos\ \alpha + \frac{\alpha}{2\ \sin\ \alpha} - 2 \tag{10}$$

3.3. Section moment produced by horizontal pressure

The buried pipe will produce the horizontal elliptical deformation subjected to the vertical earth load. The pipe's side wall

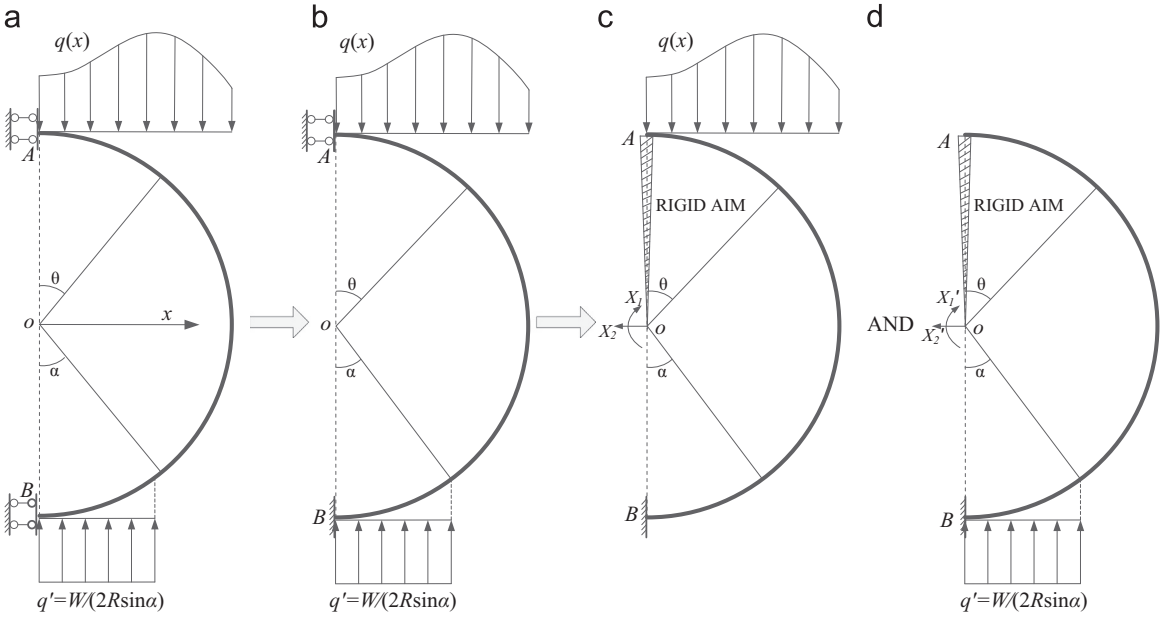

Fig. 3. Simplified mechanical model.

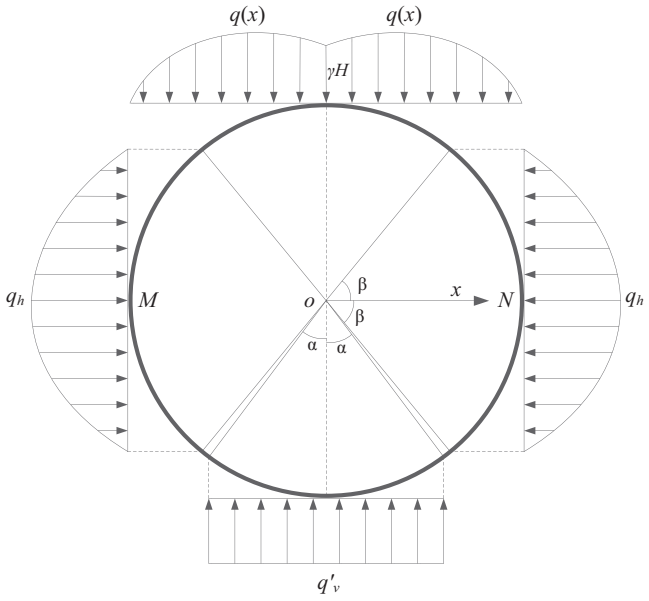

Fig. 4. New mechanical model.

protrudes outward, and passive earth pressure occurs because the backfill is squeezed. The deformation of each point on the side wall is different, and the maximum deformation occurs at the end points of the horizontal diameter (M and N, Fig. 4). Therefore, it is difficult to calculate the passive earth pressure at each point accurately. In the Spangler model, the parabolic distribution is assumed to approximately express the passive earth pressure on the pipe's side wall. In the new mechanical model, shown in Fig. 4, the parabolic distribution's assumption of the horizontal pressure is maintained.

The section moment produced by the horizontal pressure with an arbitrary range of 2β (Fig. 4) is

for $0 \le \theta \le \pi/2-\beta$:

$$M_3(\theta) = q_h R^2(3\ \sin\ \beta + \sin\ 3\beta - 6\ \sin\ \beta\ \cos\ 2\beta) \cdot [k_2(\beta) - \cos\ \theta]/\left(12\sin^2\beta\right) + M_0 \tag{11a}$$

for $\pi/2-\beta \le \theta \le \pi/2+\beta$:

$$M_3(\theta) = q_h R^2\left[48\cos^2\theta\ \cos\ 2\beta + 8\ \cos\ \theta\ \cos\ 3\theta - 12\ \cos\ 2\beta(1+\cos\ 2\theta) - 24\cos^2\theta + 3(1-\cos\ 4\theta)\right]/\left(96\sin^2\beta\right) + M_0 \tag{11b}$$

for $\pi/2+\beta \le \theta \le \pi$:

$$M_3(\theta) = q_h R^2(3\ \sin\ \beta + \sin\ 3\beta - 6\ \sin\ \beta\ \cos\ 2\beta) .(k_2(\beta) + \cos\ \theta)/\left(12\sin^2\beta\right) + M_0 \tag{11c}$$

In the above equations, M_0, $k_2(\beta)$ and q_h are expressed as follows:

$$M_0 = q_h R^2\left\{\frac{11}{32}\ \sin\ 4\beta + \frac{3\beta}{8}(3-4\ \cos\ 2\beta) - \frac{1}{2}\ \sin\ 2\beta + (3\ \sin\ \beta + \sin\ 3\beta - 6\ \sin\ \beta\ \cos\ 2\beta) \cdot \left[\cos\ \beta - k_2(\beta)\left(\pi/2-\beta\right)\right]\right\}/\left(6\pi\sin^2\beta\right) \tag{12}$$

$$k_2(\beta) = \frac{3[1-\ \cos\ 4\beta + 4\ \cos\ 2\beta\cdot(\cos\ 2\beta - 1)]}{8(3\ \sin\ \beta + \sin\ 3\beta - 6\ \sin\ \beta\ \cos\ 2\beta)} \tag{13}$$

$$q_h = e\frac{\Delta x}{2} \tag{14}$$

In Eq. (14), Δx denotes the relative displacement of points M and N, which can be determined by Eq. (22). e denotes the coefficient of passive earth pressure, N/m^3. Generally, in the analysis of buried pipes, the product of e and R is known as

$$E' = eR \tag{15}$$

where E' denotes the reaction modulus, MPa.

3.4. Maximum stress of arbitrary section

For an arbitrary section, the maximum stress can be given as follows:

$$\sigma_{\max}(\theta) = \frac{6M(\theta)}{\delta^2} \tag{16}$$

where $M(\theta)$=the total bending moment=$M_1(\theta)+M_2(\theta)+M_3(\theta)$.

4. Parabolically distributed vertical earth pressure

Shmulevich et al. (1986) performed experiments for buried steel pipes with different diameters and thicknesses in a relatively wide trench condition, which can be seen as a positive burial type. The clay and sand were selected with different degrees of compactness to use as the soil around the pipe. It is indicated that the normal and tangential soil stresses are parabolically distributed approximately above the crown of the pipe, and that the maximum values of the stresses are both in the middle. The experiment results also indicate that the tangential soil stresses are close to zero at the end points of the pipe's horizontal diameter. This finding indicates that the resultant normal and tangential stress, that is, the vertical earth pressure, is similar to the parabolic distribution, the value of which is near zero at the end points of the pipe's horizontal diameter.

Based on the above analysis, this study assumes that the vertical earth pressure is parabolically distributed and proposes a new mechanical model, as shown in Fig. 4, based on the Spangler model. The vertical earth pressure on points M and N is zero. On top of the pipe, the vertical earth pressure is set to be γH approximately, because the effect of the difference in settlement is the smallest at that point and the vertical earth pressure is the closest to the self-weight of the soil column.

As shown in Fig. 4, letting $q(x) = ax^2+bx+c$, the values for the parameters (a, b, c) can be determined from the three known conditions for any x ranging from 0 to R:

$$\begin{cases} q(0) = \gamma H, q(R) = 0 \\ \int_0^R q(x)dx = \int_0^R \left(ax^2+bx+c\right)dx = \frac{1}{2}W \end{cases} \tag{17}$$

The results are $a = -(3W-3\gamma HR)/R^3$, $b = (3W-4\gamma HR)/R^2$, $c = \gamma H$.

Substituting the results into Eqs. (7) and (8) gives the following for $0 \le \theta \le \pi/2$:

$$M_1(\theta) = \left(\frac{3}{4}RW - \frac{3}{4}\gamma HR^2\right)\sin^4\theta - \left(RW - \frac{4}{3}\gamma HR^2\right)\sin^3\theta - \frac{1}{2}\gamma HR^2\sin^2\theta + \left(\frac{1}{5\pi}RW + \frac{2}{15\pi}\gamma HR^2\right)\cos\theta + \left(\frac{7}{6\pi} - \frac{17}{64}\right)RW + \left(\frac{43}{192} - \frac{8}{9\pi}\right)\gamma HR^2 \quad (18a)$$

for $\pi/2 \le \theta \le \pi$:

$$M_1(\theta) = -\frac{1}{2}RW\sin\theta + \left(\frac{1}{5\pi}RW + \frac{2}{15\pi}\gamma HR^2\right)\cos\theta + \left(\frac{7}{6\pi} - \frac{1}{64}\right)RW + \left(\frac{59}{192} - \frac{8}{9\pi}\right)\gamma HR^2 \quad (18b)$$

$M_2(\theta)$ and $M_3(\theta)$ are still the same as in Eqs. (9) and (11), respectively.

5. Deformation formulae with vertical earth pressure parabolically distributed

In this section, the positive direction of the relative displacement is designated to be inward for the top and bottom of a pipe, and outward for the end points of the pipe' s horizontal diameter.

5.1. Relative displacement of end points of pipe's horizontal diameter

With the principle of virtual displacement, the relative displacement produced by the vertical pressure ($q(x)$ and q') is given by

$$\Delta x_v = k_{xv}\frac{R^3W}{EI} \quad (19)$$

where I is the sectional moment of inertia of the unit length of the pipe, $\delta^3/12$, and k_{xv} is the coefficient of deformation given by

$$k_{xv} = 0.1115 + \frac{k_1(\alpha)}{2\pi} - \frac{1}{12}\sin^2\alpha - \frac{0.0090}{\xi C_c}\frac{H}{D} \quad (20)$$

The relative displacement produced by the horizontal pressure is given by

$$\Delta x_h = -k_{xh}\frac{2q_hR^4}{EI} \quad (21)$$

where k_{xh} can be determined from Table 1.

Calculated by Eqs. (14), (15), (19) and (21), the relative displacement of the end points of the pipe's horizontal diameter is

$$\Delta x = \frac{k_{xv}R^3W}{EI + k_{xh}E'R^3} \quad (22)$$

5.2. Relative displacement of top and bottom of pipe

The relative displacement produced by the vertical pressure ($q(x)$ and q') is given by

$$\Delta y_v = k_{yv}\frac{R^3W}{EI} \quad (23)$$

where k_{yv} is given by

$$k_{yv} = 0.1203 - \frac{k_1(\alpha)}{2\pi} + \frac{1}{4}(\sin\alpha - \alpha) - \frac{1}{12}\sin\alpha\cos\alpha + \frac{1}{6\sin\alpha}(1 - \cos\alpha) - \frac{0.0087}{\xi C_c}\cdot\frac{H}{D} \quad (24)$$

The relative displacement produced by the horizontal pressure is given by

$$\Delta y_h = -k_{yh}\frac{2q_hR^4}{EI} \quad (25)$$

where k_{yh} can be determined from Table 2 as

Calculated by Eqs. (14), (15), (22), (23) and (25), the relative displacement of the top and bottom of a pipe is

$$\Delta y = \frac{R^3W}{EI}\left(k_{yv} - \frac{k_{xv}k_{yh}}{\frac{EI}{E'R^3} + k_{xh}}\right) \quad (26)$$

Eqs. (22) and (26) are the same as the Spangler formulae in form, and the values for k_{xh} and k_{yh} are kept the same as those in the Spangler formulae, as shown in Tables 1 and 2, respectively, and as demonstrated by Deng and Li (1998). The difference is that the values for k_{xv} and k_{yv} are changed. In the Spangler formulae, k_{xv} and k_{yv} are given by (Deng and Li, 1998), namely,

$$k_{xv} = 0.1100 + \frac{k_1(\alpha)}{2\pi} - \frac{1}{12}\sin^2\alpha \quad (27)$$

$$k_{yv} = 0.1161 - \frac{k_1(\alpha)}{2\pi} + \frac{1}{4}(\sin\alpha - \alpha) - \frac{1}{12}\sin\alpha\cos\alpha + \frac{1}{6\sin\alpha}(1 - \cos\alpha) \quad (28)$$

Comparing Eqs. (20) and (24) with Eqs. (27) and (28), it is indicated that the new formula (Eqs. (20) and (24)) captures the effects of more parameters on Δx and Δy, including H, D, C_c, and ξ.

6. Example and discussion

For a field case of a buried pipe, a circular shallow trench is excavated on a foundation in order to place the pipe. The arc angle (2α, Fig. 4) of the trench is 90°. The backfill and the foundation are silty sand. The compactness of the backfill is 90%. E_d is 10 MPa according to "GB50332-2002, Structural design code for pipelines of water supply and waste water engineering". E' is 3.5 MPa according to "GB50253-2003, Code for design of oil transportation pipeline engineering". Through static uniaxial tests and engineering experience, the elastic modulus and Poisson's ratio of the backfill are determined to be 25.72 MPa and 0.286, respectively, while those of the foundation are 81.82 MPa and 0.364, respectively.

Table 1
Value of k_{xh} for different β.

β (deg.)	40	45	50	55	60	65	70	75	80	85	90
k_{xh}	0.0544	0.0581	0.0610	0.0634	0.0653	0.0668	0.0679	0.0686	0.0692	0.0695	0.0696

Table 2
Value of k_{yh} for different β.

β (deg.)	40	45	50	55	60	65	70	75	80	85	90
k_{yh}	0.0525	0.0564	0.0596	0.0622	0.0643	0.0659	0.0671	0.0680	0.0686	0.0690	0.0691

Table 3
Parameters input into FLAC3D software.

Material (Silty sand)	Bulk modulus (MPa)	Shear modulus (MPa)	Density (kg/m^3)	Internal friction angle (deg.)	Cohesion (MPa)	Tensile strength (MPa)
Backfill	20.0	10.0	1810	29.8	0.1	0.1
Foundation	100.3	30.0	1860	34.7	0.1	0.1

The density and the internal friction angle of the backfill and the foundation are provided in Table 3. Through tensile tests, the elastic modulus (E) and Poisson's ratio (μ) of the buried steel pipe are found to be 2.0×10^{11} Pa and 0.3, respectively. The density of the steel (ρ) is 7800 kg/m^3.

Generally, to prevent the premature destruction of the soil and to obtain convergent simulation results, the two strength parameters, namely, cohesion and tensile strength, should be determined reasonably. It is found that, when the simulation is convergent, the difference in the simulation results is very small. In this article, because the two parameters for the silty sand are very small, they are selected to be the smallest values, provided in Table 3, among the many values that could ensure the convergent results.

In this section, the study selects two kinds of different outside diameter steel pipes as samples: $D=0.5$ m with $\delta=6$ mm and $D=1$ m with $\delta=10$ mm. For each kind of pipe, k_{xv} and k_{yv} are calculated for different H/D when α is 45° using the new formulae in this article, and their change curves with H/D are shown in Figs. 7–10 (New formula). In the Spangler formulae (Eqs. (27) and (28)), k_{xv} and k_{yv} are only related to α, and they are constant for different H/D. When α is 45°, the values for k_{xv} and k_{yv} are 0.09561 and 0.09662, respectively, as shown in Figs. 7–10 (Spangler formula).

In engineering, buried pipes can be simulated well using the finite difference software FLAC3D (Zhang and Zhang, 2013). In order to verify the feasibility of the new model and formulae in this article, numerical calculations using FLAC3D were conducted. The models of the foundation and the trench are shown in Fig. 5, and the overall model of the buried pipe is shown in Fig. 6. Due to the weak preprocess function of FLAC3D, the models are built and meshed with ANSYS software, and then information on the nodes and the elements

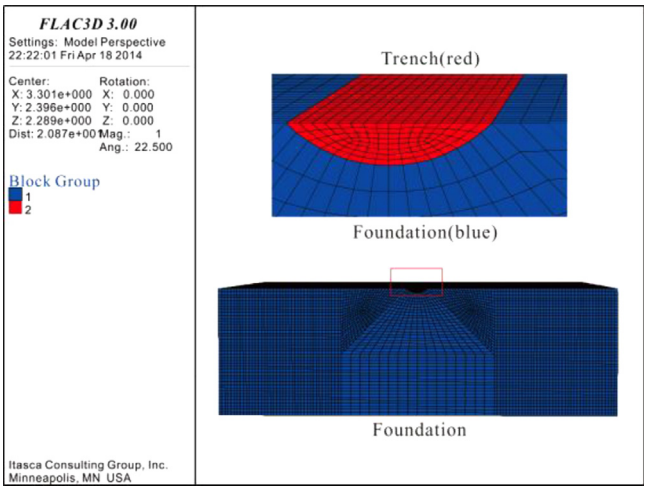

Fig. 5. Models of foundation and trench.

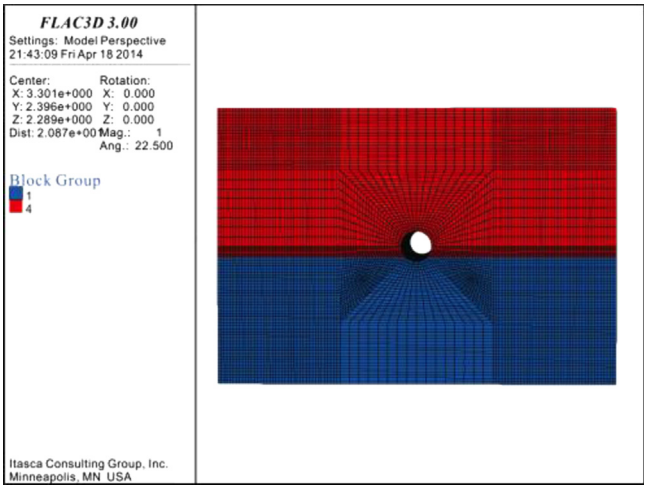

Fig. 6. Overall model of the buried pipe.

are extracted and imported into FLAC3D. A foundation, large enough in size, is adopted in the model. The height of the foundation is 4 m and it extends outward 3 m ($D=0.5$ m) and 4 m ($D=1$ m) from the left and right sides of the pipe, respectively, as shown in Fig. 5. The length of the model, that is, the length of the pipe, is selected to be 5 m.

The buried pipe can be simulated using the "shell" element provided in FLAC3D, and four parameters (E, μ, δ, ρ) should be assigned to the shell elements through command strings input into the software. For the backfill and the foundation, the adopted constitutive model in the simulation is the Mohr–Coulomb model, a kind of elastic-plastic model widely used for the simulation of soil. In FLAC3D software, the parameters shown in Table 3 are needed to simulate the soil using the Mohr–Coulomb model. The bulk modulus and the shear modulus are derived from the elastic modulus and Poisson's ratio, and the transform formulae are expressed as follows:

$$K = \frac{E_s}{3(1-2\mu_s)} \tag{29}$$

$$G = \frac{E_s}{2(1+\mu_s)} \tag{30}$$

where K is the bulk modulus, MPa; G is the shear modulus, MPa; E_s is the elastic modulus of soil, MPa; μ_s is Poisson's ratio of the soil.

As for the boundary conditions, the normal displacement of the four side faces and the bottom of the model are set to zero. The model is large enough in size, so that the boundary conditions basically coincide with the actual situation. The simulation is performed in two parts. Firstly, the initial stress state of the foundation is simulated with the model shown in Fig. 5. Secondly, the trench is excavated (the red part in Fig. 5), the shell elements and the backfill are created (Fig. 6), the parameters are assigned, and the calculation is conducted.

Through numerical calculation, the values for Δx and Δy can be obtained. Then, k_{xv} and k_{yv} can be calculated by Eqs. (23) and (28) with the known values for k_{xh} and k_{yh}, as shown in Tables 1 and 2, when β is selected to be 50°, namely, the same as for the Spangler formulae. The simulated data for k_{xv} and k_{yv} are shown in Figs. 7–10 (FLAC3D).

Figs. 7 and 8 show the data for when C_c adopts Eq. (2), while Figs. 9 and 10 show the data for when C_c adopts the American standard (Eq. (3)). It is indicated that the new formulae data agree better with the FLAC3D data, for pipes with different H/D, than the Spangler formulae data. Therefore, it is concluded that assuming a parabolic distribution results in higher accuracy than assuming the uniform distribution of the vertical earth pressure, and that the new model proposed in this article can simulate the behavior of buried pipes better than the Spangler model.

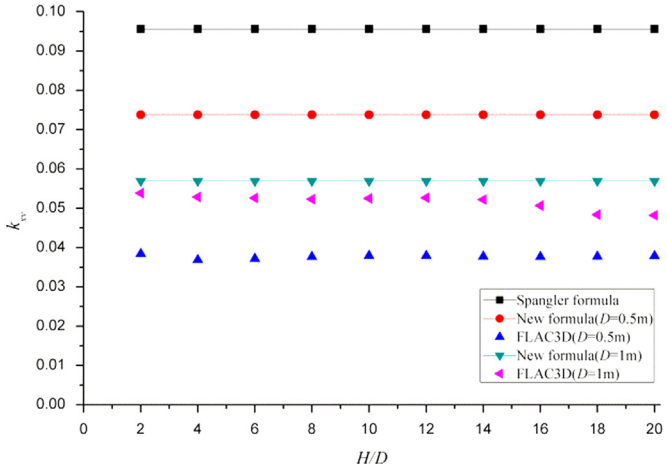

Fig. 7. k_{xv} data (C_c adopts Eq. (2)).

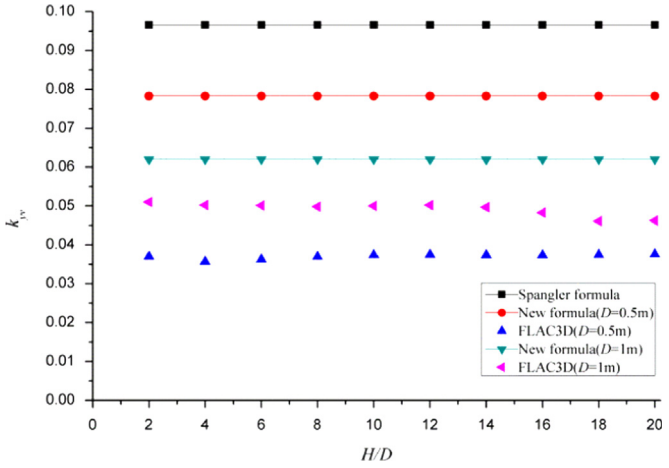

Fig. 8. k_{yv} data (C_c adopts Eq. (2)).

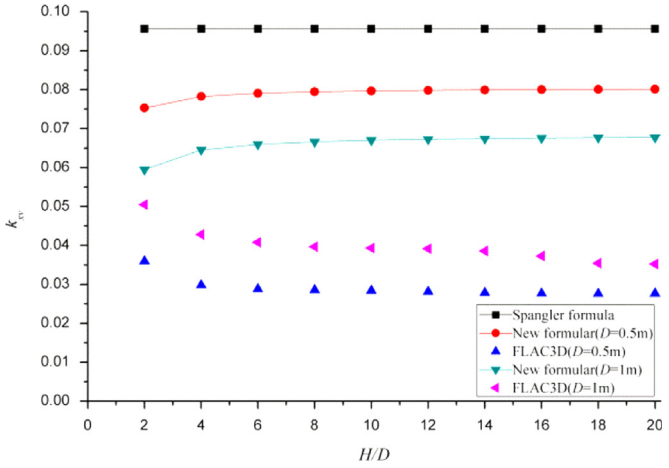

Fig. 9. k_{xv} data (C_c adopts Eq. (3)).

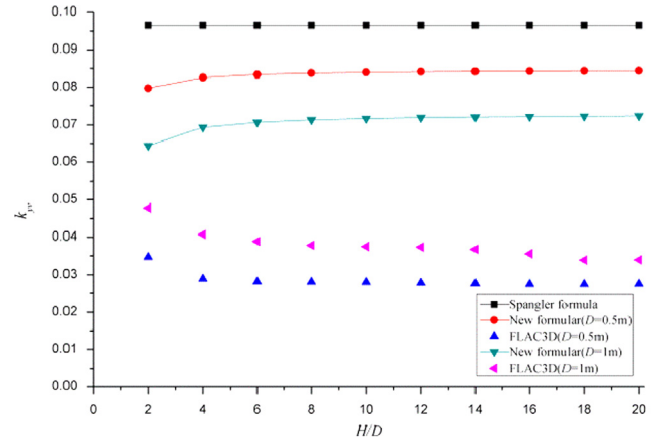

Fig. 10. k_{yv} data (C_c adopts Eq. (3)).

For the pipe $D=1$ m with $\delta=10$ mm, when C_c adopts Eq. (2), the new formulae data and the FLAC3D data are very close, and the accuracy is improved greatly compared with the Spangler formulae. When C_c adopts Eq. (3), the degree of improvement in accuracy decreases. Overall, for the two kinds of pipes, the degree of improvement for the pipe with a large diameter is greater than that for the pipe with a small diameter.

It is necessary to note that, for the pipe $D=0.5$ m with $\delta=6$ mm, the difference between the new formulae data and the FLAC3D data is relatively large, even though the accuracy of the new formulae is higher than that of the Spangler formulae. For the theoretical calculation of the new formulae or the Spangler formulae, it is difficult to consider some factors, for example, the self-weight of the pipe, the three-dimensional effects and the real pipe−soil interaction. Many assumptions and simplifications must be made which will inevitably lead to errors. When the diameter of a pipe is small, the deformation is small, and errors become relatively large.

7. Conclusions

(1) In the Spangler formulae, k_{xv} and k_{yv} are a function of single parameter α. However, through the work of this article, it is concluded that k_{xv} and k_{yv} are related to parameters H, D, ξ and C_c, but not to α.

(2) Compared with the Spangler formulae, the new formulae have higher accuracy. Assuming that the vertical earth pressure on a pipe is parabolically distributed results in higher accuracy than assuming uniform distribution. The new model proposed in this article can simulate the behavior of buried pipes better than the Spangler model.

(3) For the new formulae, when C_c adopts Eq. (2), the degree of improvement in accuracy is higher than that when C_c adopts Eq. (3). For the large-diameter pipe, the degree of improvement is larger than for the small-diameter pipe using the new formulae in this article.

(4) Although the new model and formulae proposed in this article can improve the accuracy of the calculation results, there is a difference between the results of the new formula and the results of the numerical simulation especially for the small-diameter pipe. Further research is needed on buried pipe behavior.

Acknowledgments

The authors are grateful to their colleagues, and thank them for their help and support during the different stages of this study.

References

Das, B.M., Seeley, G.R., 1975. Breakout resistance of shallow horizontal anchors. J. Geotech. Eng., ASCE 101 (9), 999–1003.

Deng, D.M., Li, Y.G., 1998. Analysis on stress and distortion of buried flexible pipeline. Oil & Gas Storage Transp. 17 (6), 57 11 − 14.

Ladanyi, B., Hoyaux, B., 1969. A study of the trap-door problem in a granular mass. Can. Geotech. J. 6 (1), 1–14.

Liu, Q.L., Yang, M., 2001. Study of vertical soil pressure on positive buried pipeline. Rock Soil Mech. 22 (2), 214–218.

Li, Y.G., 2009. Study on Unified Calculation Theory of Earth Pressure on Top of Trench-Buried Culverts and Positive-Buried Culverts Ph.D. thesis. Taiyuan University of Technology, Taiyuan.

Marston, A., Anderson, A.O., 1913. The Theory of Loads on Pipes in Ditches and Tests of Cement and Clay Drain Tile and Sewer Pipe. Iowa State College of Agriculture and Mechanic Arts, Iowa.

Meyerhof, G.G., Adams, J.I., 1968. The ultimate uplift capacity of foundations. Can. Geotech. J. 5 (4), 225–244.

Matyas, E.L., Davis, J.B., 1983a. Experimental study of earth loads on rigid pipes. J. Geotech. Eng., ASCE 109 (2), 202–209.

Matyas, E.L., Davis, J.B., 1983b. Prediction of vertical earth loads on rigid pipes. J. Geotech. Eng., ASCE 109 (2), 190–201.

Spangler, M.G., 1941. The Structural Design of Flexible Pipe Culverts. Iowa State College of Agriculture and Mechanic Arts, Iowa.

Shmulevich, I., Galili, N., Foux, A., 1986. Soil stress distribution around buried pipes. J. Transp. Eng., ASCE 112 (5), 481–494.

Tian, W.D., 1989. Review of the vertical earth pressure theory of positive buried pipe culverts in recent years at home and abroad. Zhe Jiang Hydrotech. 1, 13–21.

Tian, W.D., 1994. A discussion on computation of vertical soil pressure acting on buried pipes. Water Resour. Hydropower Eng. 3, 9–14.

Vesic, A.S., 1971. Breakout resistance of objects embedded in ocean bottom. J. Soil Mech. Found. Div., ASCE 97 (9), 1183–1205.

Zhang, Z.G., Zhang, M.X., 2013. Mechanical effects of tunneling on adjacent pipelines based on Galerkin solution and layered transfer matrix solution. Soils Found. 53 (4), 557–568.